ULTRA-WIDEBAND RADAR DEVELOPMENT FOR NON-TOUCH TERRAIN SENSING APPLICATION ON CLOSE COMBAT SUPPORT VEHICLES

(A SBIR Initiative)

Gerald V. Jung (Project Lead), Dave Fredrick, Marco C. Truong
US Army TACOM – Emerging Technologies Team
Warren, MI 48397-5000

Scott J. A. Merritts, Mitul Modi
MTU - Keweenaw Research Center
Houghton, MI 49931

Dr. Leonard S. Haynes (President), Dr. Chujen Lin, Dr. Alexander Davydov
Intelligent Automation, Incorporated
Rockville, MD 20850

Alan Petroff (VP Engineering), Larry Fullerton (Founder, CTO), Justin Hernandez
Time Domain Corporation
Huntsville, AL 35806

ABSTRACT (U)

(U) Grizzly, the Army's next-generation complex obstacle breaching system, operates in a harsh environment where sand, dirt, dust, mud, obscurants, battlefield debris, varying levels of vegetation, wide temperature ranges, and ballistic shock from artillery, direct fire, and both anti-tank & anti-personnel mine are the norm. One of the mission critical capabilities of the Grizzly is to effectively breach minefields.

(U) The US Army Tank and Automotive Research, Development and Engineering Center (TARDEC), along with the Army Research Laboratory (ARL), have a joint Phase II Small Business Innovation Research (SBIR) effort with Intelligent Automation Incorporated (IAI) to develop a novel non-touch terrain sensing technology that may be used to control the plow depth of the Grizzly's mine clearing blade (MCB). The sensor will need to determine the MCB's plow depth to within a two-inch accuracy of a user-selected depth in order to effectively clear surface and buried land mines.

DISTRIBUTION STATEMENT A
Approved for Public Release
Distribution Unlimited

20060824118

(U) The non-touch sensor approach evaluated for this application is an Ultra-Wideband (UWB) Radar array oriented to provide height and roll information necessary for the MCB to follow the terrain contour. UWB radar technology offers greater capability over other range sensors, such as laser and acoustic systems, due to its ability to "see" through dense vegetation and smoke/dust obscurants while utilizing stealthy, undetectable signals at micro-power levels.

(U) This paper presents the results of the Phase I SBIR evaluation of the UWB Radar technology as well as discussions on the Phase II SBIR development efforts of the technology into a deliverable prototype for potential application to the Grizzly MCB automatic depth control system.

(U) INTRODUCTION

(U) Grizzly, the Army's Breacher for the 21st Century, is designed to clear minefields, neutralize obstacles, demolish berms, and fill in anti-tank ditches – *"in stride"*. It is being designed by United Defense, LP (York, PA & San Jose, CA) and is based on the M1 Abrams chassis, hence, will offer the same high-level of direct fire armor protection.

(U) The four and a half-ton, mine blast survivable blade clears a 14-ft wide lane at a depth of 15 in. A crucial function to a successfully mine clearing operation is the control of the blade depth to within a 2 in accuracy. If the blade travels deeper than desired, excessive soil load may cause the vehicle to plow downwards and stall. If the blade does not plow deep enough, some buried mines may not be removed. To achieve this crucial accuracy, an Automatic Depth Control System (ADCS) is employed. The current ADCS system utilizes Tactile Depth Sensors (TDS) and Draft Force Sensors (DFS). The TDS [Fig 1] consists of three cantilevered "fingers" that folds-out over the blade. By measuring the angle of the TDS "knuckles", the variation in terrain height is attained. The DFS consists of pressure transducers on the tines. The measured pressure is compared to lookup tables of various soil types to empirically determine depth. Since

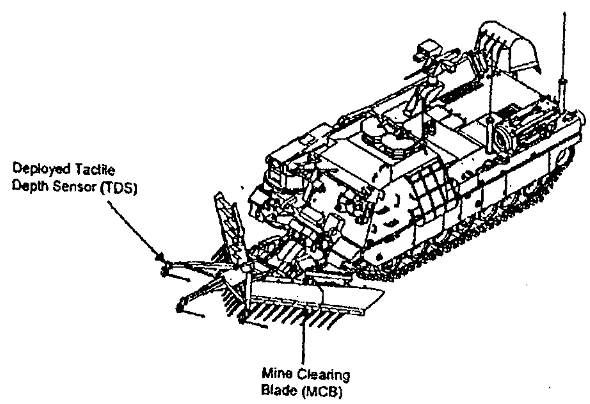

Figure 1. (U) Grizzly Breacher with TDS

both sensor suites are in front of the blade, they are susceptible to damage from exploding mines and direct fire threats.

Figure 2. (U) One of 3 HyDRAs

(U) The Emerging Technologies Team at TARDEC has been working with PM-Grizzly to develop a second generation Automatic Depth Control System. Our first concept solution is the Hybrid Damage Reduction Abatement (HyDRA) system [Fig 2]. The system was developed earlier this year and will be tested on the Grizzly vehicle this summer. The HyDRA consists of an array of three armored, charged-couple device triangulating lasers mounted above and back behind the blade. An air-knife overpressure system ensures the laser optics remain dust-free. The system works by emitting high-speed laser pulses (667 pps), where some of the pulses would penetrates between the foliage & debris to accurately range the distance to the soil. This information is then used to precisely control the blade depth. Although lasers are highly accurate (+/- 0.001 in), they do require a direct line-of-sight to the target. Hence, heavy foliage would block the laser's view to the soil surface. Also, lasers cannot penetrate surface water accumulations (i.e. puddles).

(U) The topic of this paper is our second concept solution using Time Modulated, Ultra-Wideband Radar (TM-UWB). This technology has the ability to "see" the ground through foliage, water, and even rocks. In 1998, a Phase I Small Business Innovation Research (SBIR) was awarded to Intelligent Automations, Inc (IAI) to evaluate the capability of this technology for terrain sensing application. This year, a Phase II SBIR was awarded to IAI to develop a prototype TM-UWB radar terrain sensing system for testing on the Grizzly. IAI's technology partner is Time Domain Corp (TDC) who holds the core patents to the TM-UWB technology.

(U) *The Technology*[1]*:*

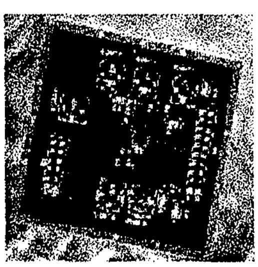

Figure 3. (U) ASIC

(U) The two enabling technologies for practical application of time-modulated, ultra-wideband radar are: 1) high-speed, digital switches capable of creating very fast rise-time and ultra-short duration pulses and 2) high-speed digitally-controlled, low-powered oscillators that can precisely measure the time of flight of the RF pulses to within 10 picosecond resolutions. In 1998, Time Domain Corp designed and had IBM fabricate the Timing Delay Generator ASIC chip based on a Silicon Germanium substrate. Later that year, IBM delivered to TDC the Multiple Correlator ASIC chip [Fig 3]. A third chip should be completed this year that will perform the digital signal processing. With this silicon trio, portable, low-power TM-UWB radar, communication, and geo-positioning devices will soon be a reality.

(U) TDC has demonstrated their technology by building a radar system, the RadarVision 1000, that is capable of "seeing" through walls & rocks to detect people and movement for law enforcement and emergency rescue units (FEMA). This is the radar used for our Phase I evaluation. For Phase II development, we will be using their new soon-to-be-released PADDS system which is a research, development and prototyping platform capable of controlling three simultaneous RF channels. They also built and demonstrated the feasibility of Low Probability of Detection (LPD) / Low Probability of Intercept (LPI) radios for the US Marine Corp which not only provided secure communication, but also position location of each radio unit to within inches [Fig 4]. An inherent feature of TM-UWB technology is accurate geo-positioning that can be used to track fire fighters or SWAT teams as well as location of cargo. Since most of the front-end technology resides on three chips, the costs for these products will be low once mass-produced.

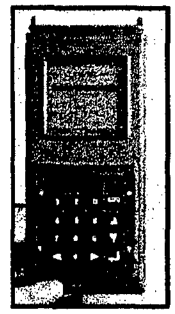

Figure 4. (U) LPI/LPD Radio for USMC

(U) TM-UWB radar technology differs from conventional radar in two significant ways. First, the radio waves are not continuous, but rather ultra-short impulses (0.5 ns pulse widths - ½ ft wavelength) [Fig 5]. These "gaussian monocycles" are inherently ultra-wide band in frequency. The center frequency of the impulse wave is approximately the reciprocal of the pulse width and the bandwidth is approximately 116% of the center frequency. Therefore, a 0.5 ns pulse width will have a center frequency of 2 GHz and a half-power bandwidth (-3 dB) of 2.32 GHz – hence, ultra-wideband. Second, for communication applications, the data signal is modulated in time instead of in amplitude (AM) or frequency (FM). The digital "1" or "0" is determined by placing the wave pulse either 100 ps earlier or later (i.e. +/- 1 in offset) than the nominal pulse repetition time (avg. interval between pulses is 100 ns).

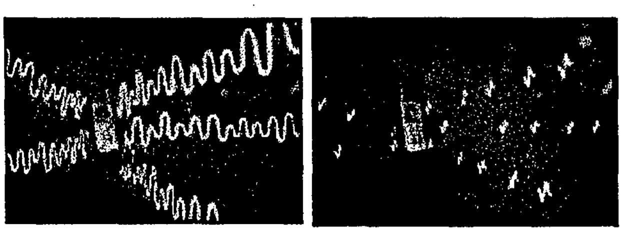

Figure 5 - Traditional Continuous Wave vs. Pulse

(U) In order to distinguish individual signals from multiple UWB radars/radios, each receiver/transmitter pair is channelized by varying the time duration between pulses in accordance with a predetermined repetition pattern using pseudo-random noise (PN) code algorithms. A matched correlating receiver "looks" for the expected pulse pattern in the "noise" of RF signals generated from other surrounding sources. This correlation is performed on a pulse-by-pulse bases within 10 ns. With a pulse-to-pulse width of 100 ns and a pulse timer accuracy of 10 picoseconds, there are 10,000 theoretically possible channels.

(U) The radio frequency (RF) emissions are also undetectable and unjammable. The power for UWB transmissions are typically in the order of 0.00001 Watt compared to current cell phone power of 0.3-1.0 W. The 0.01 mW energy is also spread across a 2 GHz bandwidth of frequency. The extremely low energy levels make it difficult to detect above that of background

radiation. Even if one is looking for the signal in the background noise level, it would be nearly impossible to determine which part of the signal is information versus noise without knowing the PN code pattern.

(U) One of the greatest advantages of pulse technology is the minimization of multi-path effects that plagues continuous wave transmissions. Once the cross-correlator achieves transmitter/receiver lock and detects the first pulse pattern, any subsequent reception of multi-pathed pulse patterns are ignored. In fact, a system employing a raked antenna design with multiple correlators can purposely listen for the subsequent multi-path pulses to increase the signal gain.

(U) Phase I SBIR[2]

(U) *Objectives:*

(U) The objective of the Phase I SBIR was to evaluate the potential of using TM-UWB radar for terrain sensing applications. IAI & TDC conducted the evaluation using the RadarVision 1000 [Fig 6, Tbl I]. It is a commercial product developed by TDC for law enforcement to "see" people through walls and doors [Fig 7].

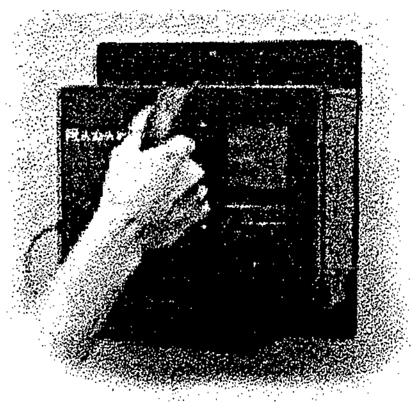

Table I. (U) Performance Specifications

Characteristic	Spec
Optimum Range	0 – 20 ft
Detection Velocities	0.5 – 15 fps
Power Source	2 hr Rech Battery
Weight	14 lbs
Center Frequency	2.0 GHz
Bandwidth (3 dB)	1.4 GHz
Range Resolution	4.5 inches
Transmit Power	0.01 mW
Antenna Gain	6 dBi
Effective Radiated Power	0.04 mW EIRP
Code Span	25 ns
Code Length	1001 chips
Nominal Pulse Rep. Rate	5 MHz
Field of View (Azm / Elv)	120 x 100 degs
Min. Target Sensitivity	-10 dBsm

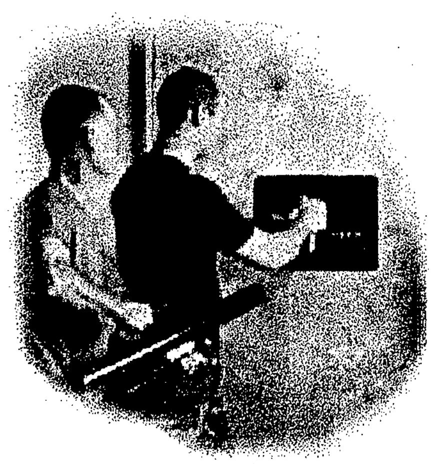

Figure 7. (U) Detection Through Walls

(U) The radar was evaluated on how well it penetrated through various terrain covers. Terrain types ranged from low growing patchy grass to thick bushes and rocky fields. We also evaluated its ability to range through dense smoke.

(U) *Test Methodology:*

(U) To facilitate test setup at the various terrain locations, the RadarVision 1000 was mounted behind a van, aimed directly downwards. A laptop computer in the van was all that was need to capture the radar's "A" scan wave forms.

(U) *Field Test Results:*

(U) The phase I SBIR test results exceeded all expectations and were highly conclusive. Two configurations were tested and both series of tests verify the feasibility and effectiveness of the terrain sensing sensor. The first configuration tested assumed that the radar antennas would be mounted in exactly the same place as the current tactile sensors, facing down at the ground. The second series of tests measured the ability of the sensor to be mounted looking forward of the vehicle, thereby allowing it to be mounted behind the Grizzly blade for greater blast protection while still providing range data. This second series of tests was surprisingly successful, yielding a 30 degree look-ahead angle with a single sensor. As will be described in detail later, by putting a reflector plate in front of the antenna to reflect signals from unwanted angles, any forward look angle may be achieved without using phased array techniques. The 30 degree look ahead angle was achieved with no plate in front of the antenna. Look ahead angles of 60 degrees may be achievable. It may be possible to achieve any angle, but more experimentation would be required to confirm this conjecture.

(U) Greater look-ahead angles and higher spatial resolution could also be achieved with phased array techniques. Detailed simulations were done using the Grizzly geometry for sensor placement. High spatial resolution at any forward look angle can be achieved with only software to fuse the data from three to possibly six transmit/receive pairs.

(U) Figure 8 shows an example of a typical return signal profile. The horizontal axis can be thought of as range to the target, or equivalently, can be thought of as the time of flight of the impulse from the antenna, to the ground, and back to the antenna. The initial ringing on the left of the trace is an artifact of the electronic coupling of the transmit and receive antennas. It is identical in every case and is ignored. The reflection of the signal off the ground is clearly visible. Each tick mark represents ½ foot. Later tests have the output formatted differently and show that we achieved .1 inch resolution. The measurements shown in this proposal were with

no calibration of any kind, and represent the worst case. Calibration and some optimization of the electronics could achieve even better results.

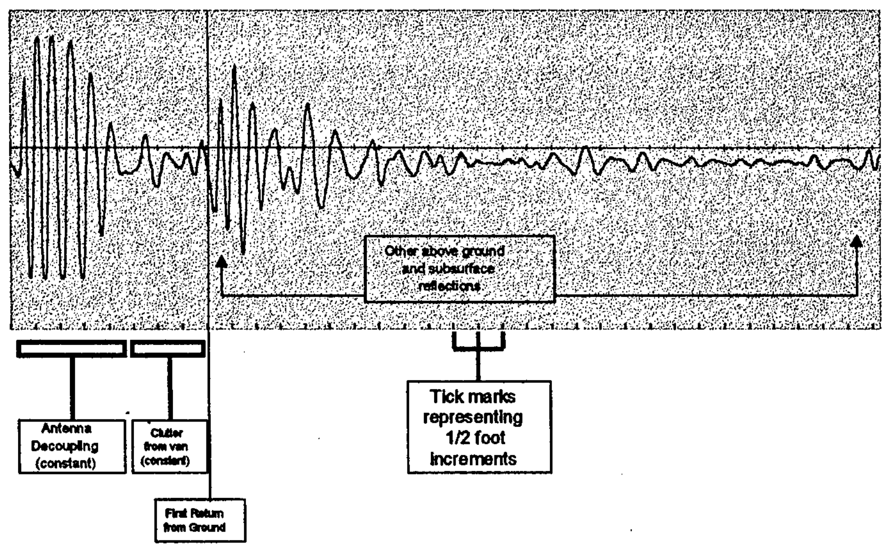

Figure 8. (U) Typical 'A' Scan Range Profile

(U) Figure 9 shows a simple case with the sensor mounted on the back of a van. The return from the ground is obvious and the reading is within 0.1 inch of the absolute measure. In all these measurements, a large attenuator (over 20 dBs) was used because at these short ranges, far too much signal was returned.

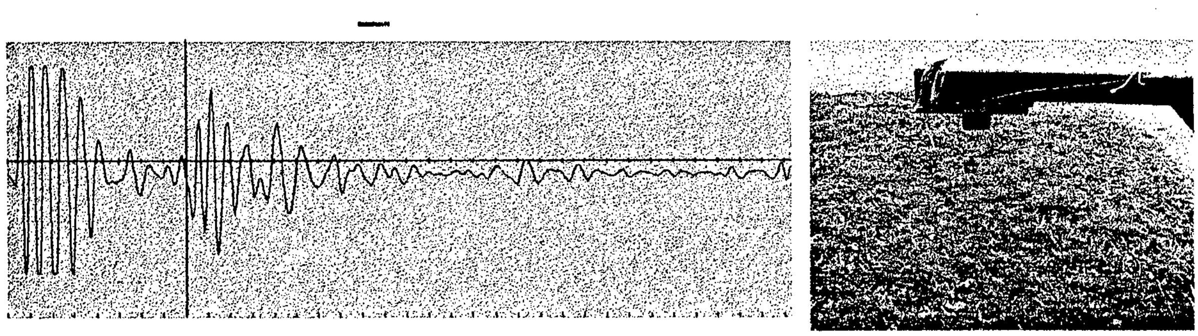

Figure 9. (U) Return Trace Over Low Grass

(U) Figure 10 and 11 shows the radar making measurements through dense smoke, as may be encountered when the Grizzly is performing a combat mission. The two radar returns shown are with and without the smoke, and are identical. The smoke makes absolutely no difference in the measurement.

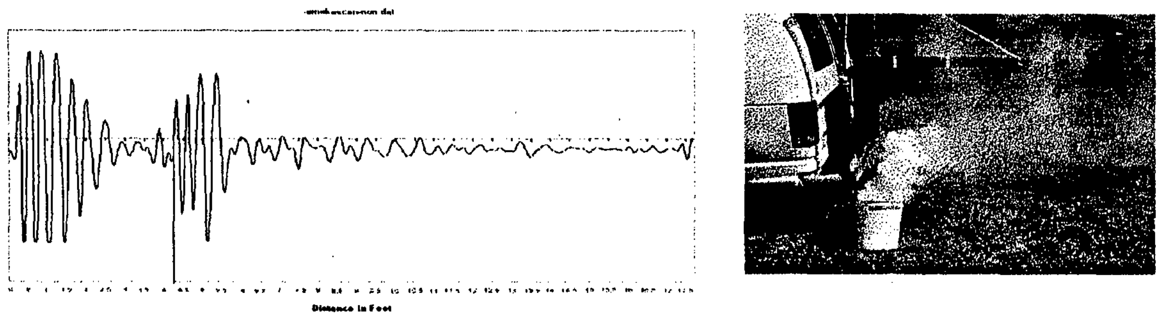

Figure 11. (U) Trace of Ground Profile with No Smoke Obscurants

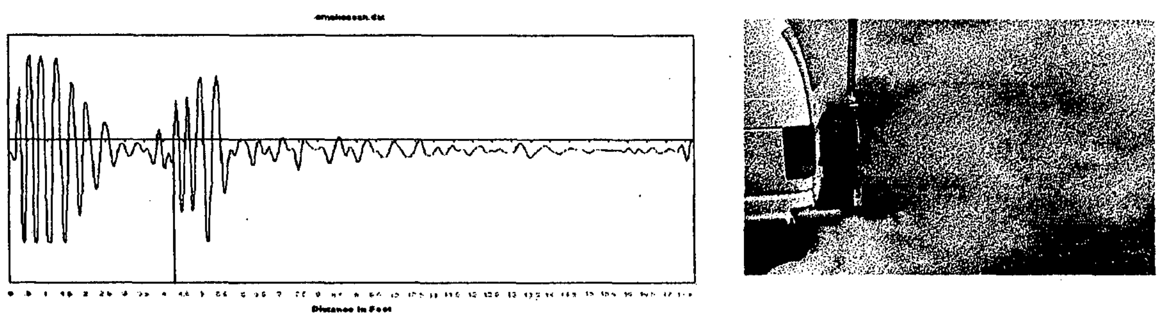

Figure 10. (U) Trace with Dense Smoke Obscurant

(U) Figure 12 and 13 shows the case where the same measurement was made with and without a huge pile of foliage between the ground and the antennas. The reading is also unchanged between these two measurements (i.e., with and without the foliage).

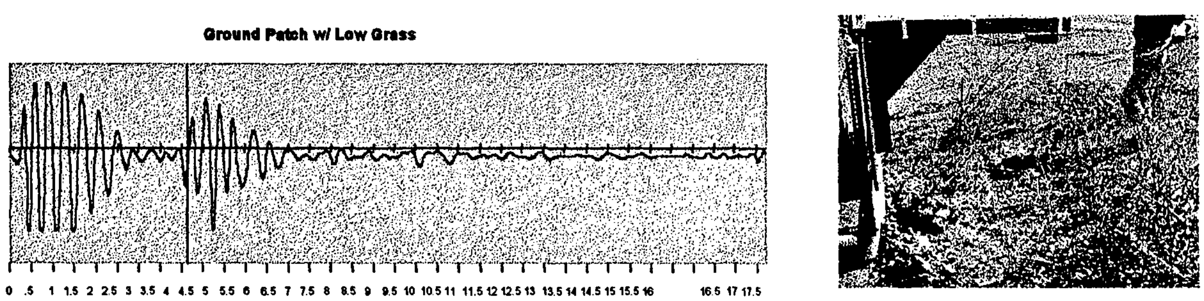

Figure 12. (U) Trace of Ground Thin Brush

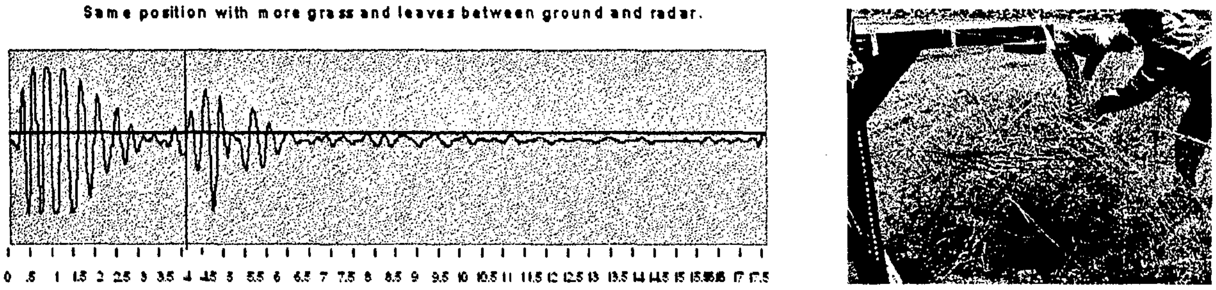

Figure 13. (U) Trace of Ground with Dense Brush

(U) ***Laboratory Results – Reflector Tests:***

(U) The Grizzly will often encounter mines. The plow and main vehicle body is designed to survive the blast, but the current tactile sensors would not survive the blast. It was a major goal of the Phase 1 work to demonstrate that the terrain sensing radar could survive a near direct blast. The best way to achieve that goal is to position the sensor behind the plow so that the plow will shield the sensor from the full strength of the blast. The following test data show that our TM-UWB sensor can achieve the desired look-ahead angles, even without the use of Phased Array techniques.

(U) The issue of the survivability of the Grizzly terrain mapping sensor is a critical issue. TM-UWB has a unique property that kevlar (what bulletproof vests are made from) is transparent to TM-UWB RF transmissions. This means that we can cover the sensors with even inches of kevlar with minimal attenuation of the signal. With the sensor mounted behind the plow, and a kevlar cover over the antenna elements, the sensor should be able to survive most blasts which the plow blade would survive. During the Phase II work, we will fabricate the kevlar covers for the antenna elements.

(U) There are two ways for the sensor to have a forward look angle. The first is by physically putting reflectors in front of and/or around the antenna to create a directional beam. With very little experimentation we obtained a 30 degree forward look angle. One of the experiments strongly suggests that because the signal to noise ratio is so high (we used a 20 dB attenuator to avoid saturating the electronics) any forward look angle could be achieved by putting a metal shield in front of the antenna where returns are not desired, leaving only the angles where returns are desired. The experiments and results are given in this section.

(U) The second way that the GTMS could achieve a forward look angle is by fusing multiple antenna data together to create a phased array. The original concept was to use three sensors to independently replace the three tactile sensors now on the Grizzly, but by combining the three

signals with the correct fixed delays, we can achieve a very narrow beam which could be aimed at any angle forward of the Grizzly. Analysis and simulation results are given below. In short, with a 6 foot base distance, easily achievable on the Grizzly, a 2 degree beam width can be achieved. This means that if the antenna were physically aimed at 60 degrees, with a 2 degree beam width, the effective look angle from the Grizzly forward would be 59 degrees. The simulations done on this are shown in this the next section.

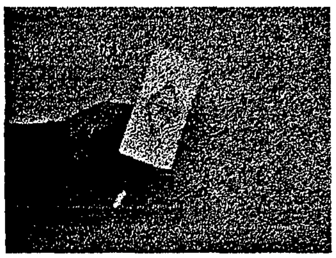

Figure 14. (U) Dipole Antenna

(U) Our description of the work done starts with the antenna, which is shown in Figure 14. It is a simple dipole, and emits or receives energy in approximately a spherical shape around the antenna. Figure 15 and 16 shows the antennas augmented with a corner reflector, which reflects the RF energy, creating a more directed beam of sensitivity.

(U) The following figures show our prototype horizontally [Fig 15] and vertically [Fig 16] polarized transmit/receive pairs. The reflector redirects energy from undesirable directions to create a narrower response shape. Horizontally and vertically polarized configurations are then made by the relative placement of these antenna modules. There are many other configurations to try since the basic antenna element shown in Figure 14 is not symmetric. The reflectors could have been rotated 90 degrees with respect to the basic dipole, but there was no time to experiment with these other options. The results obtained, then, could be significantly improved upon with additional experimentation.

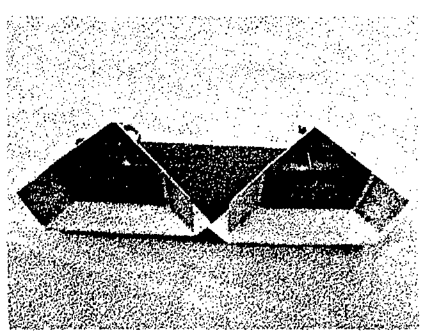

Figure 15. (U) Horizontally Polarized Transmit/Receive Antenna Pairs

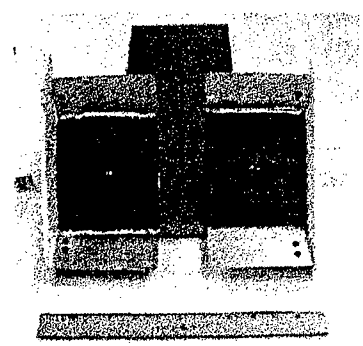

Figure 16. (U) Vertically Polarized Transmit/Receive

(U) Figure 17 shows the experimental setup to obtain the beam pattern of the horizontally polarized antenna configuration. The target, shown in the figure, is moved through the scene, and the regions where the target is detected are mapped. In some regions the corner reflectors have eliminated the emitted signal, or eliminated the received signals, and in those areas, there is no response. The ideal beam pattern would be one that is very narrow. Figure 18 shows the beam pattern for the horizontally polarized transmit/receive antenna configuration.

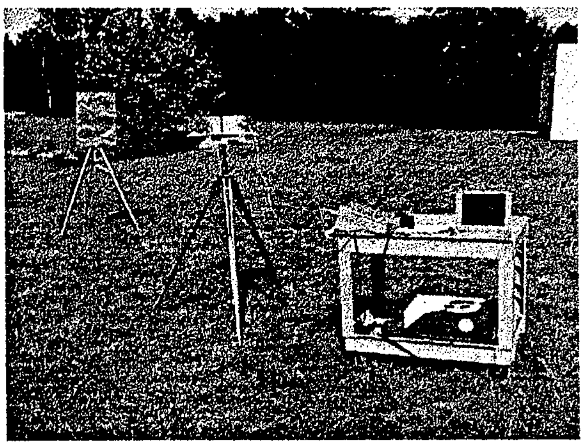

Figure 18. (U) Horizontal Antenna Field Strength Profile Setup

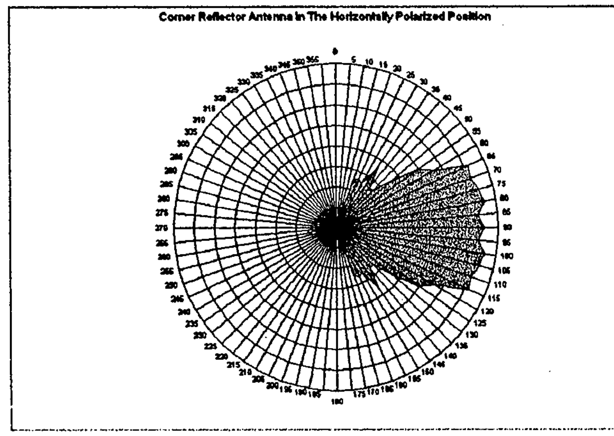

Figure 17. (U) Beam Pattern for Horizontally Polarized Antenna Pair

(U) Figure 19 shows the setup for the final series of tests, where we verified the actual forward look angle achieved. The antenna was mounted as shown, and measurements were made. Since the floor is at a continuously increasing distance from the antenna, the distance actually returned will be the range to the closest point on the floor where the system has response. This will be the hypotenuse of the triangle made up of the height of the antenna, the range (which is the

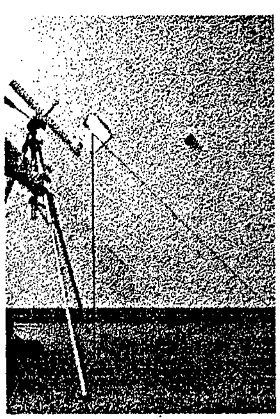

Figure 19. (U) Antenna Pair with Reflector Plate

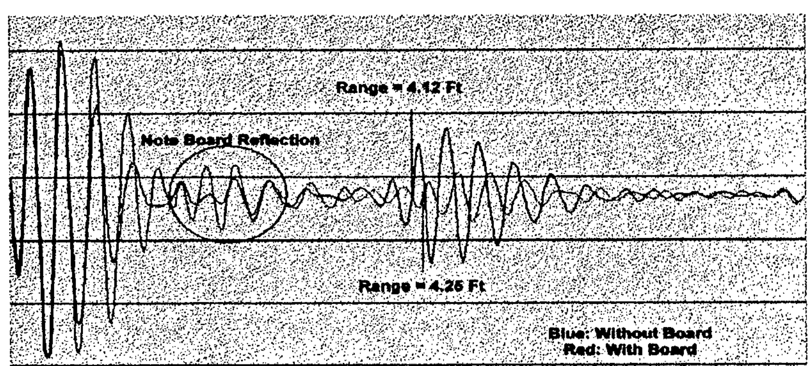

Test Results	Off Axis Range	Effective Forward Look Angle
Without Reflective Board	12 inches	14 degrees
With Reflective Board	13.5 inches	15.75 degrees

Figure 20. (U) Trace With and Without Reflector Board

hypotenuse), and the forward look distance. The arctan of the height over the range of the antenna gives the forward look angle, and the forward look distance (the horizontal distance in front of the antenna to which we are measuring) is the height of the antenna times the tangent of the forward look angle. The results are shown in Figure 20. In this figure we see an effective forward look angle of 14 degrees. IAI suggested to TDC that by using a metal plate to block part of the filed into which the emissions would normally propagate, any angle could be achieved easily with the current sensor.

(U) ***Modeling & Simulations - Phased Array Techniques:***

(U) Reflectors offer a purely passive way to achieve the desired Grizzly sensor look-ahead angle. There are also simple ways that multiple sensor signals can be fused purely in software to create very narrow beams. Phased array techniques can be done in hardware also, and that allows more energy to be focused on a target in a specific direction. It also allows the antenna to receive more energy from a given direction. In our case, there is a factor of 10 too much signal, and we intentionally attenuate the received signal. As a result of this abundance of signal, mathematically delaying and adding signals is just as effective as actually delaying the transmitted and received signals, and is much easier and more flexible. A narrow beam can be created mathematically and used to mathematically scan the ground to learn specific terrain details such as holes, slope, etc.

(U) During Phase I, we were limited in what we could do in this area, but we did perform several simulations of mathematically delaying and adding signals from multiple antennas. The results were encouraging. We have used a tool that simulates TM-UWB radar imaging. Figure 21 shows three emitter/receivers. The size of the dots shown represents the wavelength of the monopulse used for the simulation, and the distance between the emitter/receivers is to scale with the distance to the scene. The geometry used matches what we would use in the Grizzly. The beam formed from the coincidence of the signal from the three emitter/receivers at one range is shown in Figure 22. The gain in power is 9 to 1 with the three emitter/receivers.

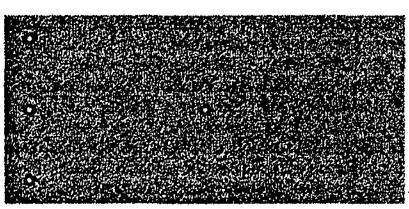

Figure 22. (U) Simulation of Three Emitter/Receiver Pairs

Figure 23. (U) Intensity of Phased Array Signal

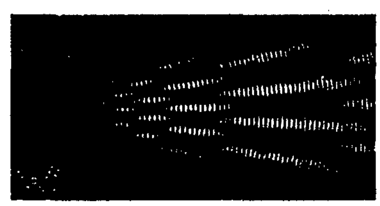

Figure 21. (U) Interference Pattern of a Continuous Wave

(U) Figure 23 very graphically shows why pulse modulated radar is so much easier to use for beam forming than conventional radar. The figure shows the points where the beams coincide

for the 6 emitter/receiver pair case in conventional radar where a carrier frequency is being generated. The many coincident points occur because there are multiple cycles generated, any of which can add constructively with any other. The single point of constructive interference for impulse radar becomes a huge number for conventional radar.

(U) Government Tests[3]

(U) Upon conclusion of the Phase I SBIR, the Terrain Sensing Laboratory (TSL), under the Emerging Technologies Team, had a two week window to conduct additional testing on the RadarVision 1000. The tests conducted by IAI and TDC produced encouraging results. The TSL wanted to investigate some of the test areas more thoroughly to gain additional insight as well as verify some of the key performance claims. A field test plan was developed to: (1) Quantify the relationship between the return signal strength with respect to changes in target range, elevation & azimuth; and (2) Quantify the relationship between the return signal strength and various types of ground cover. Each of the following questions could also be resolved in the course of investigating the above two relationships:

1) (U) Maximum/Minimum Operating Range
2) (U) Range Accuracy
3) (U) Repeatability
4) (U) Field of View
5) (U) Field Strength
6) (U) Ability to Penetrate Various Ground Covers
7) (U) Multipath Immunity
8) (U) Co-site Interference
9) (U) Vibration Tolerance
10) (U) Shock Tolerance
11) (U) Calibration & PMCS
12) (U) Effects of Horn, Wave Guide & Reflectors
13) (U) Ability to Penetrate Various Atmospheric Conditions (e.g. rain, snow, sleet, fog)
14) (U) Ability to Operate in Temperature Extremes

(U) The first week was devoted to exploratory lab tests to gain familiarity with the radar. Due to the limited space in our laboratory, it was difficult to conduct any tests greater than 5' before running into clutter from either the floor or ceiling. The second week was devoted to outdoor testing were we would have greater free (uncluttered) space. Two field test setups were required to explore all the issues above.

(U) *Test Setup A – Relationship Between Signal Strength and Target Location*

(U) Test Setup A [Fig 24] was used to investigate the relationship between the return signal strength versus target position in range, elevation and azimuth with respect to the transmit

antenna's center beam width axis. The RadarVision 1000 display software is hard-coded for an operating range between 0-20 ft. The first 2-3 ft of range is ambiguous do to coupling effects between the transmitter and receiver antennas. Therefore, we selected the test range to be between 5 – 20 ft in increments of 5 ft. In order to obtain accurate and repeatable results, we needed to ensure that the test environment was free of clutter. Although we could not avoid extraneous background RF noise from nearby broadcast and cellular towers, we could control the ground clutter. The RadarVision 1000's user manual specifies the FOV to be 120° in Azimuth and 100° in elevation. To ensure all ground clutter was avoided, the radar was elevated to 55° above horizon. To ensure a consistent target cross sectional area throughout the test and to aid in the determining of the precise distance between the radar and the first return point on the target, an approximately one-foot diameter aluminum sphere was used as the target. The target was created by wrapping aluminum foil around a soccer ball. Lab tests showed that the return signal strength is highly sensitive to the incident angle on the target. To ensure sufficient return signal, the aluminum foil was evenly crumpled prior to placement over the ball.

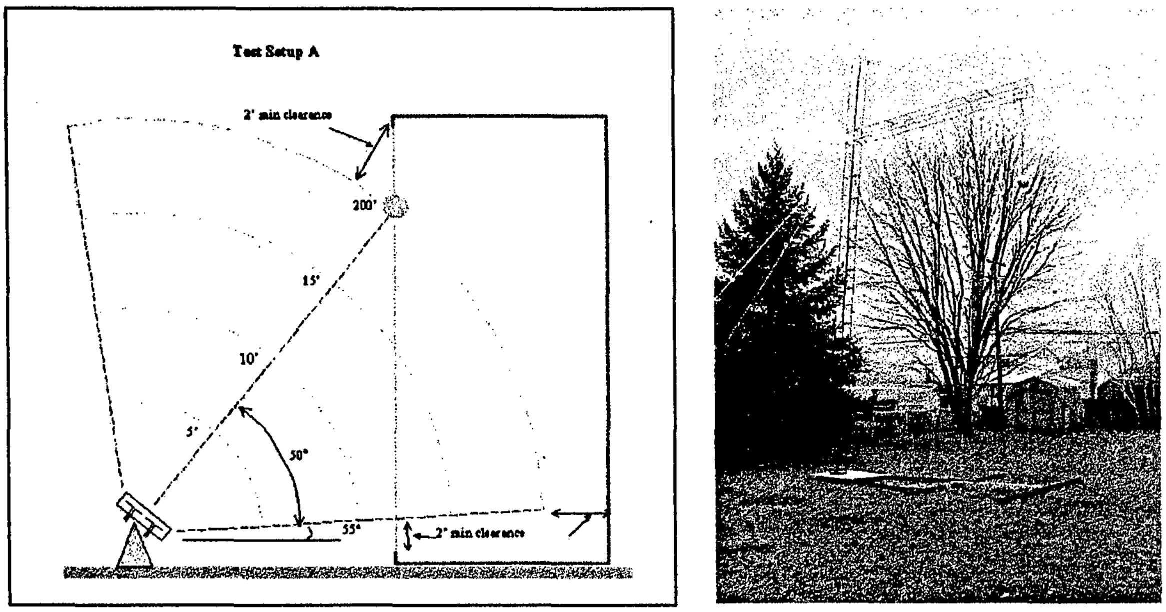

Figure 23. (U) Test Setup A

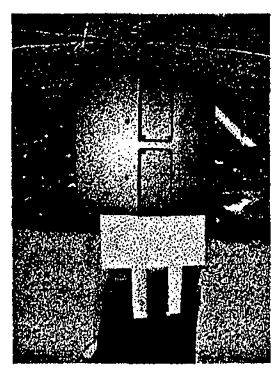

Figure 25. (U) Antennas & Back plate Detached From Processor Box

(U) The spherical target was attached to a RF transparent, low-stretch nylon rope attached to a gantry. The gantry was designed and orientated in such a manner to guarantee a 10% minimum range separation between the target and the gantry.

(U) The transmit and receive antennas, along with the back scatter plate, were detached from the signal processor box and attached to a telescope mount to provide precise azimuth adjustments [Fig. 25]. The signal processor box was located near the laptop that contained

Figure 24. (U) Adjusting Angle and Range for Each Test

the data collection and analysis software provided with the RadarVision 1000. Since the radar's elevation was fixed at 55° (to avoid ground clutter), the radar's elevation relative to the target was adjusted by raising and lowering the target [Fig 26]. The target height was determined by measuring the length of rope between the target and the ground. One foot ticks were marked on the rope. A ruler attached to the base support provided the inch-resolution measurements between the 1 ft ticks. There was low stretch and vibration in the rope so the height of the target could be calculated to within +/- 1 inch.

(U) To acquire the field strength at various ranges, the antenna mount was moved radially outwards, in 5' increments, from the base of the gantry. Elevation varied from –55° to 55° with respect to the radar's central beam axis to target. Azimuth varied from –67° to 67°. The extremes of these ranges were selected to verify the radar's specified FOV [Tbl II].

Table II. (U) Field of View & Range Permultations

Range	5'	10'	15'	20'							
Elevation	-55°	-50°	-35°	-20°	-10°	0°	10°	20°	35°	50°	55°
Azimuth	-67°	-60°	-45°	-30°	-15°	0°	15°	30°	45°	60°	67°

(U) There are a total of 484 permutations of the above combinations. To reduce the magnitude of the test trials required to adequately characterize the radar's field strength, only "strips" of data were taken. Imagine a 3D hemispherical shell, like the top half of a globe of the earth from the equator up with the North Pole at the top of the shell. The radius of the shell/globe represents the range. For our tests, we chose a radius of 15'. On the perimeter of this shell are three arcs (strips) spaced 45° apart that start from the center of the shell and runs down to the base edge of the hemisphere. This would be similar to the 0°, 45° and 90° longitudinal lines of our globe. The interval between these elevation and azimuth measurement points are give in the chart above. These three strips of data are sufficient to characterize one quadrant of the radar's FOV. To verify the assumed symmetry of the dipole antenna, several data points were taken in the other three

Table III. (U) Setup A Data Collection Sheet

UWB RADAR SETUP A
TEST DATA COLLECTION SHEET

Date: Start Time: Stop Time: Temp: Humidity:

Range: 5'		Measured	Range: 10'		Measured	Range: 15'		Measured	Range: 20'		Measured
Ang Off Axis	Azimuth	Range	Ang Off Axis	Azimuth	Range	Ang Off Axis	Azimuth	Range	Ang Off Axis	Azimuth	Range
-55	-67		-55	-67		-55	-67		-55	-67	
	-60			-60			-60			-60	
	-45			-45			-45			-45	
	-30			-30			-30			-30	
	-15			-15			-15			-15	
	0			0			0			0	
	15			15			15			15	
	30			30			30			30	
	45			45			45			45	
	60			60			60			60	
	67			67			67			67	
-50	-67		-50	-67		-50	-67		-50	-67	
	-60			-60			-60			-60	
	-45			-45			-45			-45	
	-30			-30			-30			-30	
	-15			-15			-15			-15	
	0			0			0			0	
	15			15			15			15	
	30			30			30			30	
	45			45			45			45	
	60			60			60			60	
	67			67			67			67	
-35	-67		-35	-67		-35	-67		-35	-67	
	-60			-60			-60			-60	
	-45			-45			-45			-45	
	-30			-30			-30			-30	
	-15			-15			-15			-15	
	0			0			0			0	
	15			15			15			15	
	30			30			30			30	
	45			45			45			45	
	60			60			60			60	
	67			67			67			67	
-20	-67		-20	-67		-20	-67		-20	-67	
	-60			-60			-60			-60	
	-45			-45			-45			-45	
	-30			-30			-30			-30	
	-15			-15			-15			-15	
	0			0			0			0	
	15			15			15			15	
	30			30			30			30	
	45			45			45			45	
	60			60			60			60	
	67			67			67			67	
-10	-67		-10	-67		-10	-67		-10	-67	
	-60			-60			-60			-60	
	-45			-45			-45			-45	
	-30			-30			-30			-30	
	-15			-15			-15			-15	
	0			0			0			0	
	15			15			15			15	
	30			30			30			30	
	45			45			45			45	
	60			60			60			60	
	67			67			67			67	
0	-67		0	-67		0	-67		0	-67	
	-60			-60			-60			-60	
	-45			-45			-45			-45	
	-30			-30			-30			-30	
	-15			-15			-15			-15	
	0			0			0			0	
	15			15			15			15	
	30			30			30			30	

quadrants at locations corresponding to points in the first quadrant where the bulk of the data was taken. Also, several data points were taken for each of the other three ranges, corresponding to the locations of the first quadrant data for our 15' range baseline shell. The data collection sheet on the right indicates the representative points collected [Tbl III]. We were able to reduce the amount of data points required down from 484 to a manageable 46.

(U) ***Test Setup B – Relationship Between Signal Strength and Various Ground Clutter***

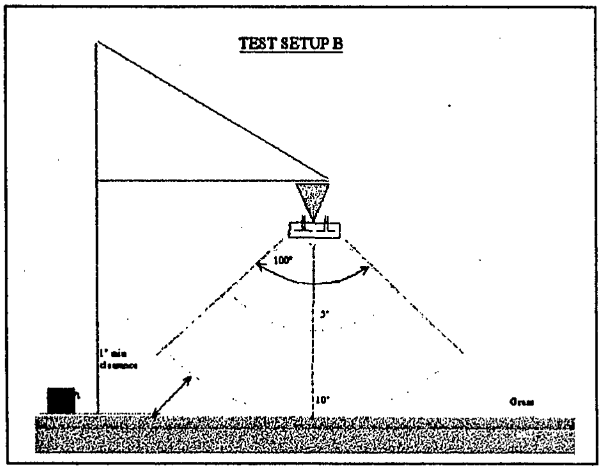

Figure 24. (U) Setup B - Ground Cover Characterization

(U) Test Setup B [Fig. 26] was used to determine the attenuation ability of various ground clutter. The following ground clutter was to be evaluated:

1. (U) Clay Soil (baseline)
2. (U) * Plastic Wading Pool (used to transfer ground clutter to the test location)
3. (U) Grass*
4. (U) Fresh Leaves*
5. (U) Dry Leaves*
6. (U) Sand*
7. (U) Puddle*

(U) The radar antenna was mounted half-way along a 14'-2"x4" plank that was suspended by two 10' ladders. The ground clutter material was transferred from a tarp into a small wading pool (i.e. children's play pool). The pool was brought under the radar antenna. After each trial, the material was dumped back onto the tarp, The pool was rinsed and dried before the next material was transferred in. Tests were done for both dry and wet ground cover [Tbl IV].

Table IV. (U) Data Collection Sheet for Setup B

APPENDIX C

UWB RADAR SETUP C

TEST DATA COLLECTION SHEET

Date: ______ Start Time: ______ Stop Time: ______ Temp: ______ Humidity: ______

Height to Ground 15' Material Thickness > 4" Wet ~ Fully Soaked

Material	Thickness	Dry	Wet
Grass			
Tarp			
Fresh Leaves			
Dry Leaves			
Soil			
Sand			
Puddle			

(U) ***Field Test Results:***

(U) Unfortunately, due to a series of problems, our field data is inconclusive. However, we did gather a host of lessons learned. Prior to each day's test, we would calibrate the RadarVision 1000 [Fig. 28]. The calibration software detects movement at what it thinks is five feet. As our calibration target, we manually vibrated a wheeled tool chest at the five foot range mark. We

adjusted the software off-set until the software detected the movement. Through this calibration test, we estimated the accuracy of the radar to be +/- 1 in.

(U) We dismounted the transmit and receive antenna from the 14 lb processor box and mounted the antenna, along with the back scatter plate that the antennas were mounted on, to a telescope tripod. We replaced the original 1' cable that connected the antennas to the processor box with a 25' shielded, low-resistance cable. However, because of the longer time required for the signal to travel through the cable to the processor box, the processor would time-out (stop listening for the signal) before the pulse signal finally arrives to the box. We were hoping that this would simply show up as a distance offset our software, but unfortunately, the maximum range window was only 20' and the cable added too much additional time/range. The shorter cable made it impossible to conduct the Materials Penetration Test under Test Setup B. The Signal Field Strength Test, under Setup A, was still doable although awkward with the shorter cable since the antenna mount was not designed to hold the entire RadarVision 1000 unit.

Figure 28. (U) Calibration

(U) We conducted several baseline tests with the target in the same location, however, the return signal traces kept changing and there appeared to be substantial background clutter [Fig 29] which we were hoping to have avoided but elevating the center of the antenna beam width axis 55° above the horizon. After many checks and cross-checks, we determined that the sidelobes of the radar was actually greater than the spec'ed 120° azimuth x 100° elevation and was actually greater than 180°. Also, the two antenna pass through holes on the back of the back scatter plate provided a path for the radar to detect the operator's movement directly behind the radar. The RadarVision 1000 was original designed for the antenna and back scatter plate to be mounted against the metallic cover of the processor unit thereby covering the "leakage" from the antenna through holes. Also, the unit was designed to be pressed flush against a wall or door to detect movement on the other side. The radar unit has two modes: a scan mode that picks-up all signal returns and a difference mode that only picks-up movement. We were using the scan mode so all returns were received and the target was masked in the clutter noise. When we switched to the difference mode, we were able to pickup two distinct targets: the actual intended target and the operator shaking the rope that the target was attached to. Provided we ensured both targets were in different ranges, we could isolate the intended target signal. However, this gave us only range data and not our desired signal strength data. Also, we could not use this mode to determine an accurate range because the target had a vibration amplitude of approximately 18". Since we had already

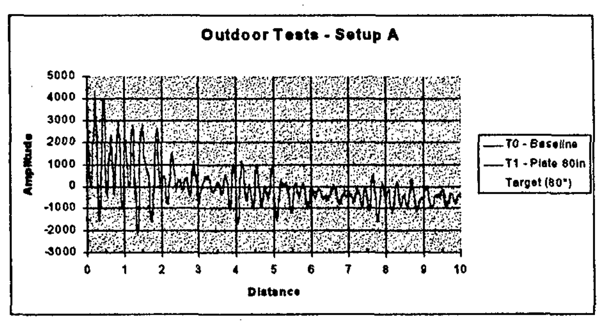

Figure 29. (U) Test Indicates Background Clutter

determined the radar's accuracy through controlled lab tests, this information was not very useful.

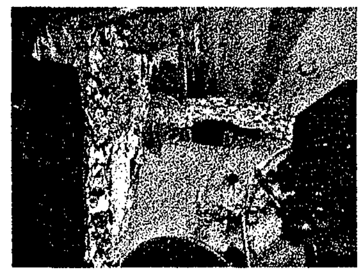

Figure 30. (U) Foil Shielding Over Back Plate Holes and Antenna Cables

(U) We decided to stay with the scan mode, but first, we shielded the pass through holes on the back scatter plate with aluminum foil [Fig. 30] and to put a 6" deep, rectangular aluminum air duct over the antenna's to help narrow the field of view [Fig. 31]. This resulted in very strong ghost targets at various ranges. We believe the RF energy was bouncing back and forth off the parallel walls of the duct before intercepting the receiver antenna, hence giving strong, but false ghost targets.

Figure 31. (U) Rectangular Duct Over Antennas

(U) We next decided to fabricate a horn using aluminum foil over cardboard panels. One test determined that the radar was sensitive enough to detect a moving target behind a thin sheet of aluminum foil. Hence we decided to make the horn panels with 2-plys to aluminum foil. The panels were mounted in the rectangular duct at an angle – like a horn. Again, there were ghost images from this configuration, through not as pronounced. It was determined that by smoothing flat the two plies of aluminum foil, the amount of ghost image and their ranges would reduce. It is hypothesized that the RF signal could have been reflecting between the two plies of aluminum foil before reflecting out and entering the receiving antenna [Fig 32]. A ply was removed and the horn was reassembled with just 1-ply panels. The signal had slightly less lower amplitude ghost images, but there were still several large amplitude images. It was noticed that the assembly of the four panels that made-up the horn altered the images significantly. We believe the RF signal may have "leaked" between the seams of the four panels and reflected around in the base rectangular duct before bouncing back through the seams and hitting the receiving antenna. Because we could not guarantee the horn assembly would not shift, we had no way of isolating and ignoring the ghost images.

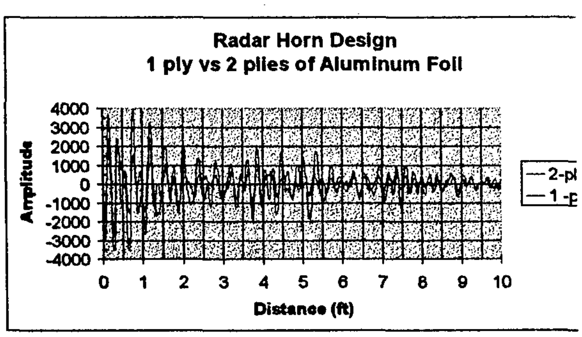

Figure 32. (U) One Ply vs. Two Ply Aluminum Foil Horn Design

(U) During our last day of test, the radar stopped functioning. It was later determined by TDC that the radar built up an internal static electric charge that fried a circuit. TDC said that this problem was common during operations in cold dry air. They said that they have fixed this problem in their new design by replacing most of the discrete circuit components (i.e. transistors, resisters, and capacitors) with two newly developed ASIC chips. During one test, we brought the radar indoors after being exposed to sub 50° temperature. It was noticed that the relative

amplitude of a signal profile does not chance, but there is an offset [Fig 33]. The colder the temperature of the radar unit, the further away from the y zero crossing the range profile lies. Also noticed that at colder temperatures, the profiles has a slight downward slope.

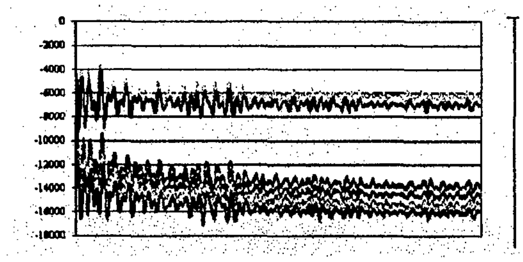

Figure 33. (U) Temperature Affects Trace Offset

(U) *Indoor Lab Tests:*

(U) Prior to the field tests, we conducted several preliminary indoor tests to get a feel of the radar's capabilities. However, due to the high clutter within the lab environment, it was extremely difficult to obtain unambiguous results beyond a range of 5' (distance to ceiling or floor).

(U) The first test we conducted was to evaluate the radar's range accuracy. Our target was a rectangular aluminum plate oriented directly towards the antennas. We incrementally advanced the target in 2" increments starting from 5' to 4' radially from the antennas. The data was superimposed on the following plot [Fig 34].

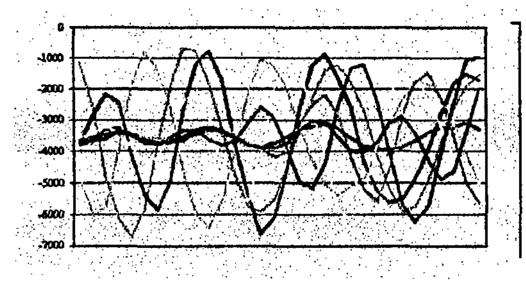

Figure 34. (U) Accuracy Test

(U) The x-axis represents the range. A plot shows a range window of 4-5 feet with the 4 ft mark on the left side. Since the calibration process requires a vibrating target, we could only ascertain the accuracy of the start of the range window to within 1 in of the actual range. Therefore, we took the distance to the peak of the first range profile as the baseline for all subsequent target range measurements.

Table V. (U) Accuracy of Each Range Trace

	RANGE MEASUREMENTS		
Profile Color	Tape Measure	Radar	Difference (in)
Red	60.00	60.00	0.00
Green	58.00	57.97	-0.03
Blue	56.00	56.08	0.08
Yellow	54.00	54.09	0.09
Purple	52.00	51.50	-0.50
Cyan	50.00	49.80	-0.20
Gold	48.00	47.72	-0.28

(U) As you can see by the following table [Tbl V], our accuracy was within ½" with 2/3 of the range measurements within ¼". We also noticed a shift in phase from one target profile to the next. The radar processor appears to shift the first major peak of the return signal to correspond the where the target starts.

(U) Our final lab test was to evaluate the radar's sensitivity to various target types. Targets included an aluminum foil covered soccer ball, a aluminum foil covered 1' square plate, an empty CD case. As the following plot [Fig 35] indicates, only the plate produced a significant return signal. The other targets only provided small amplitude changes in at the 4.5' target range.

(U) Since we erroneously assumed the radar's field of view was 120° by 100°, per spec, we could not guarantee the radar was not picking up background clutter which may have masked the signal from the smaller radar cross sectional area targets.

(U) During the differential mode, where the radar senses changes in the environment's signature, even a small 4" diameter steel ball, rolling from 15' away, could easily be detected.

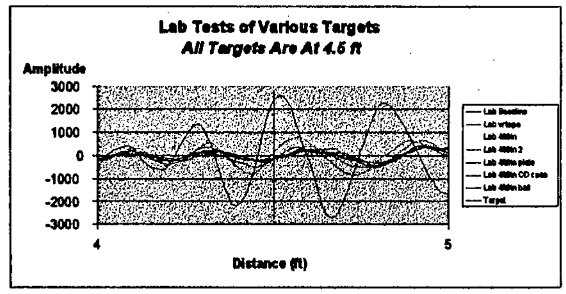

Figure 35. (U) Relative Cross Sectional Areas of Various Targets

(U) PHASE II SBIR EFFORTS

(U) During the Phase II SBIR, IAI and TDC will apply the lessons learned in Phase I to develop a customized terrain sensing radar package that could be integratable onto the Grizzly as a complementary sensor suite to the HyDRA laser ranging system. Work efforts will focus on achieving 50° look-ahead angles (measured looking directly down and turning upwards towards the horizon. Look-ahead capability will allow the radar to be located safely behind the Grizzly blade.

(U) Development emphasis will be placed on antenna design to narrow the beam width from the current 120° x 100° to at least 30°. Wave guides and reflector plates will also be evaluated. The last development thrust will be to evaluate and develop a multi-antenna, phased array system. Although the last approach would be the most complicated to design and implement, the production cost should still be modest since only one set of the ASIC chips could handle the processing of multiple antenna returns. The antennas are also low cost.

(U) One of the first tasks of this phase will be to complete the characterization of the radar field strength and the attenuation ability of various ground covers that was initiated during the government test portion of the Phase I SBIR.

(U) CONCLUSION

(U) Intelligent Automation Incorporated, along with the technology partner, Time Domain Corp, produced excellent results from the Phase I SBIR. Although the government had limited

success with it's evaluation of the radar, due to the limited test time and learning curve, the data that we were able to obtain, as well as the superb results from IAI and TDC, clearly shows the viability of Time Modulated, Ultra-Wide Band Radar for terrain sensing applications.

(U) We were able to validate the accuracy of the range resolution to ¼" and, with more precise and controlled tests in the future, we are sure we will be able to achieve the $^{1}/_{10}$" claims of the contractor. We were able to accurately "see" through heavy vegetation such as bushes, leaves, and branches. We were also able to "see" through dense smoke.

(U) Using a reflector plate with the standard "wide" FOV antenna, we were able to achieve a 30° look-ahead angle. A more focused antenna design as well as proper reflector placement should easily increase our look-ahead angle to our 50°.

(U) We do not foresee any difficulties with the maturation of the terrain sensing radar. IAI has a strong research team with supportive management. Partnered with TDC, the visionary inventors of UWB technology, we are confident that by the conclusion of this two year, Phase II SBIR contract, we will have a fully-functioning terrain sensing radar ready for testing and implementation on the Grizzly – the Army's 21st Century Breacher.

(U) REFERENCES:

(U) [1] Petroff, A. and Withington, P., *Time Modulated Ultra-Wideband (TM-UWB) Overview*, Wireless Symposium/Portable by Design, February 2000.

(U) [2] Haynes, L.S., Petroff, A., Hernandez, J., *Ultra-Wideband Radar Terrain Mapping Sensor Phase I SBIR Final Report,* Phase I SBIR UWB Radar Deliverable, May 1999.

(U) [3] Jung, G.V., *UWB-Radar Government Test Plan,* Phase I SBIR UWB Radar Project Management, December 1999.

16271

OPSEC REVIEW CERTIFICATION

(AR 530-1, Operations Security)

I am aware that there is foreign intelligence interest in open source publications. I ave sufficient technical expertise in the subject matter of this paper to make a etermination that the net benefit of this public release outweighs any potential damage.

Reviewer: STEVEN J McCORMICK GS-13 MECHANICAL ENGINEER

Name Grade Title

Steven J McCormick 21 MAR 00

Signature Date

Description of Information Reviewed:

Title: ULTRA-WIDER and Radar Development for Non-touch Terrain Sensing Application on Close Combat Support Vehicles

Author/Originator(s): Gerald Jung, Dave Fredrick, Marco Truong

Publication/Presentation/Release Date: 27 March 2000

Purpose of Release: 11th Annual US Army Conference

A bstract, summary, or copy of the information reviewed is available for review.

Reviewer's Determination (check one)

✓ 1. Unclassified Unlimited.

2. Unclassified Limited, Dissemination Restrictions IAW ______

3. Classified. Cannot be released, and requires classification and control at the level of ______

Security Office (AMSTA-CM-XS):

Concur/Nonconcur [signature] 21 Mar 00

Signature Date

Public Affairs Office (AMSTA-CM-PI):

Concur/Nonconcur [signature] 3/21/00

Signature Date

STA 7114-E
Sep 1999

Please call Lisa Anderson at 45951 for pickup. Thanks